Design of a Ruthenium-Labeled Cytochrome *c* Derivative to Study Electron Transfer with the Cytochrome bc_1 Complex†

Gregory Engstrom,‡ Ray Rajagukguk,‡ Aleister J. Saunders,§ Chetan N. Patel,§ Sany Rajagukguk,‡ Torsten Merbitz-Zahradnik,|| Kunhong Xiao,⊥ Gary J. Pielak,§ Bernard Trumpower,|| Chang-An Yu,⊥ Linda Yu,⊥ Bill Durham,‡ and Francis Millett*,‡

Department of Chemistry and Biochemistry, University of Arkansas, Fayetteville, Arkansas 72701, Department of Chemistry, University of North Carolina, Chapel Hill, North Carolina 27599-3290, Department of Biochemistry, Dartmouth Medical School, Hanover, New Hampshire 03755, and Department of Biochemistry and Molecular Biology, Oklahoma State University, Stillwater, Oklahoma 74078

Received November 20, 2002; Revised Manuscript Received January 23, 2003

ABSTRACT: A new ruthenium-cytochrome *c* derivative was designed to study electron transfer from cytochrome bc_1 to cytochrome *c* (Cc). The single sulfhydryl on yeast H39C;C102T iso-1-Cc was labeled with Ru(2,2′-bipyrazine)$_2$(4-bromomethyl-4′-methyl-2,2′-bipyridine) to form Ru_z-39-Cc. The Ru_z-39-Cc derivative has the same steady-state activity with yeast cytochrome bc_1 as wild-type yeast iso-1-Cc, indicating that the ruthenium complex does not interfere in the binding interaction. Laser excitation of reduced Ru_z-39-Cc results in electron transfer from heme *c* to the excited state of ruthenium with a rate constant of 1.5×10^6 s^{-1}. The resulting Ru(I) is rapidly oxidized by atmospheric oxygen in the buffer. The yield of photooxidized heme *c* is 20% in a single flash. Flash photolysis of a 1:1 complex between reduced yeast cytochrome bc_1 and Ru_z-39-Cc at low ionic strength leads to rapid photooxidation of heme *c*, followed by intracomplex electron transfer from cytochrome c_1 to heme *c* with a rate constant of 1.4×10^4 s^{-1}. As the ionic strength is raised above 100 mM, the intracomplex phase disappears, and a new phase appears due to the bimolecular reaction between solution Ru-39-Cc and cytochrome bc_1. The interaction of yeast Ru-39-Cc with yeast cytochrome bc_1 is stronger than that of horse Ru-39-Cc with bovine cytochrome bc_1, suggesting that nonpolar interactions are stronger in the yeast system.

The cytochrome bc_1 complex (cyt bc_1)[1] is an integral membrane protein in the energy-conserving electron transport chains of mitochondria and many respiratory and photosynthetic prokaryotes (*1*). The complex contains cyt c_1, the Rieske iron−sulfur protein, and two *b*-type hemes (b_L and b_H) in the cyt *b* subunit (*1*, *2*). Electron transfer through the complex is thought to involve a Q-cycle mechanism in which protons are translocated from the negative to the positive side of the membrane as electrons are transferred from ubiquinol to cytochrome *c* (Cc) (*2*). Cc is a small water-soluble heme protein that transfers electrons from the cyt bc_1 complex to cytochrome *c* oxidase by a diffusional shuttle mechanism (*3*, *4*). The electron-transfer reaction from the cyt bc_1 complex to Cc involves at least three steps: formation of a 1:1 reactant complex between reduced cyt bc_1 and Cc^{3+}, intracomplex electron transfer from cyt c_1^{2+} to Cc^{3+}, and release of Cc^{2+}. The interaction between Cc and cyt bc_1 should be optimized to allow rapid electron transfer in the reactant complex, as well as facilitate rapid reactant complex formation and product complex dissociation. The overall reaction rate measured by both steady-state and stopped-flow kinetics decreases with increasing ionic strength, indicating that the interaction has an electrostatic component (*3*−*8*). Chemical modification studies have suggested that six lysine amino groups surrounding the heme crevice of Cc are involved in the interaction with cyt bc_1 (*3*, *4*, *6*−*9*). Likewise, chemical modification and cross-linking studies have implicated acidic residues on bovine cyt c_1 in binding Cc, as well as acidic residues on subunit 8, called the hinge protein (*10*−*12*). The X-ray crystal structures of beef, chicken, and yeast cyt bc_1 show that the cyt c_1 heme edge on the cytoplasmic surface is surrounded by acidic residues that could form a docking site for Cc (*13*−*16*). The X-ray crystal structure of the complex between yeast Cc and yeast cyt bc_1 has recently been determined to 2.97 Å resolution (*17*) (Figure 1). The most remarkable feature of this structure is that the complex is stabilized largely by nonpolar interactions, including a planar stacking interaction between yCc Arg-13 and Phe-230 of cyt c_1. Complementary charged residues are located around the periphery of the binding

† This work was supported by NIH Grants GM20488 (F.M. and B.D.), GM30721 (C.-A.Y.), and GM20379 (B.T.).

* To whom correspondence should be addressed. Fax: (479) 575-4049. Phone: (479) 575-4999. E-mail: millett@comp.uark.edu.

‡ University of Arkansas.

§ University of North Carolina, Chapel Hill.

|| Dartmouth Medical School.

⊥ Oklahoma State University.

[1] Abbreviations: cyt bc_1, cytochrome bc_1; Cc, cytochrome *c*; yCc, yeast Cc; Ru_z-39-Cc, Ru(bpz)$_2$dmb-Cys-39-(H39C;C102T)-yCc; Ru_p-39-Cc, Ru(bpy)$_2$dmb-Cys-39-(H39C;C102T)-yCc; bpy, 2,2′-bipyridine; dmb, 4,4′-dimethyl-2,2′-bipyridine; bpz, 2,2′-bipyrazine; TMPD, tetramethylphenylenediamine; 3CP, 3-carboxy-2,2,5,5-tetramethylbyrrolidine-*N*-oxyl; $Q_0C_{10}Br$, 2,3-dimethoxy-5-methyl-6-(10-bromodecyl)-1,4-benzoquinol.

10.1021/bi027213g CCC: $25.00
Published on Web 02/22/2003

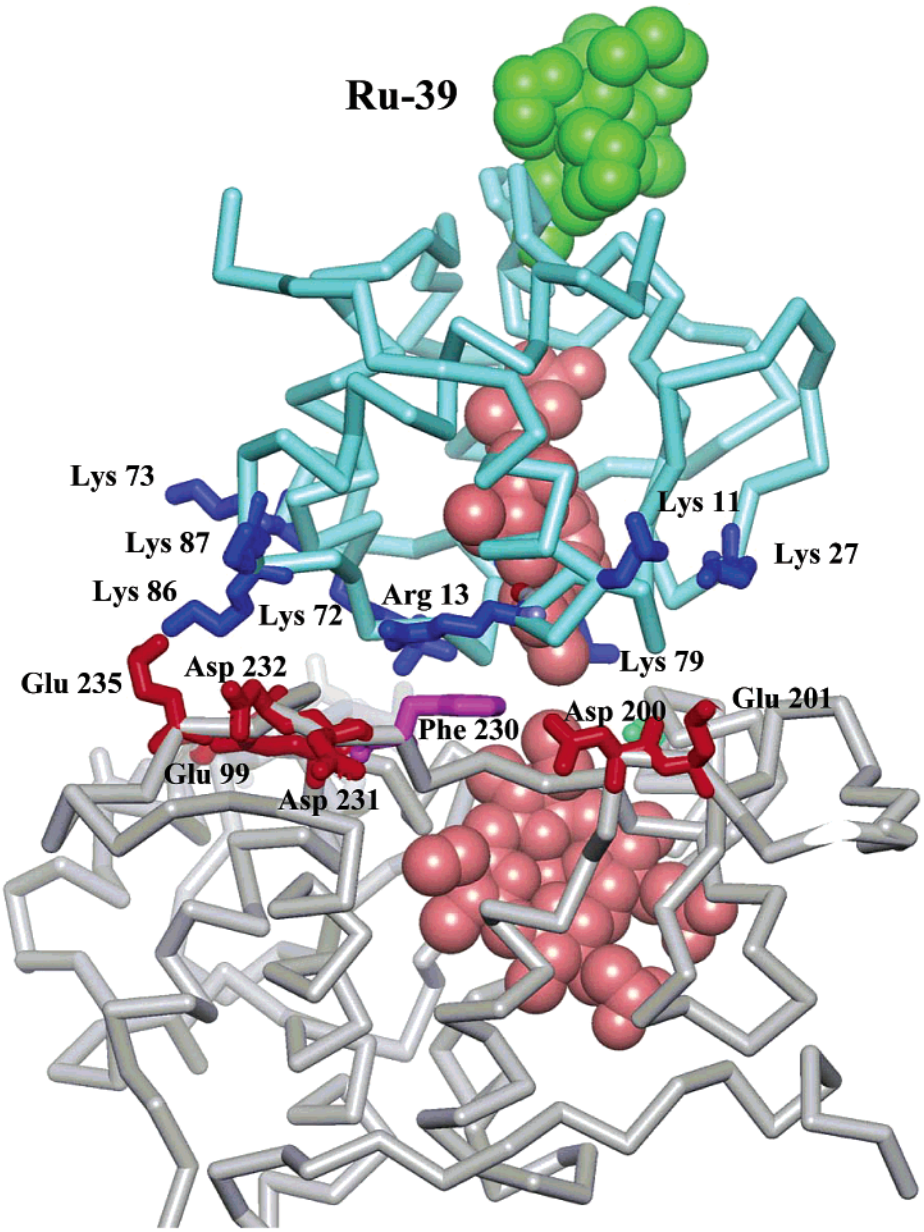

FIGURE 1: X-ray crystal structure of the complex between yeast cyt bc_1 and yCc (*17*). Cyt c_1 is colored gray, yCc is light blue, the heme groups are pink, acidic residues on cyt c_1 are red, basic residues on yCc are blue, and Phe-230 is purple. The ruthenium complex on Cys-39 is green.

domain, but only two are close enough to potentially make direct polar interactions. The distance between the edges of the heme *c* and heme c_1 groups is only 9.4 Å, giving an estimated rate constant for electron transfer of 1×10^6 to 8×10^6 s^{-1} (*17*).

In this investigation, a new ruthenium-Cc derivative has been designed to study electron transfer from cyt c_1 to Cc. A new brominated $Ru(bpz)_2(dmb)$ reagent was synthesized and used to label the sulfhydryl group on yeast H39C,C102T Cc to form Ru_z-39-Cc (Figure 1). The Ru_z-39-Cc derivative has the same steady-state activity with yeast cyt bc_1 as native yeast iso-1-Cc, indicating that the ruthenium complex does not interfere in the binding interaction. The $Ru(bpz)_2(dmb)$ complex is particularly effective for photooxidation of the reduced heme in Ru_z-39-Cc, with a rate constant of 1.5×10^6 s^{-1} and a yield of 20% in a single flash. This new complex, which has not been previously used in biological electron-transfer studies, may be useful for other applications requiring efficient photooxidation of redox centers. Flash photolysis of a 1:1 complex between reduced yeast cyt bc_1 and Ru_z-39-Cc at low ionic strength leads to rapid photooxidation of heme *c*, followed by intracomplex electron transfer from cyt c_1 to heme *c* with a rate constant of 1.4×10^4 s^{-1}. This is the first experimental measurement of intracomplex electron transfer from cyt c_1 to Cc in the yeast complex and is interpreted with reference to the X-ray crystal structure of the yeast Cc:cyt bc_1 complex. As the ionic strength is raised above 100 mM, the complex dissociates, and the bimolecular reaction between solution Ru_z-39-Cc and cyt bc_1 is observed. The ionic strength dependence of the kinetics indicates that nonpolar interactions between yeast Ru-39-Cc and yeast cyt bc_1 are quite strong, consistent with the X-ray crystal structure. By comparison, nonpolar interactions are not as strong in the complex between horse Ru-39-Cc and bovine cyt bc_1.

EXPERIMENTAL PROCEDURES

Materials. Yeast cyt bc_1 was purified as described by Snyder and Trumpower (*18*). Bovine cyt bc_1 was purified as described by Yu et al. (*19*), while *R. sphaeroides* cyt bc_1 was purified as described by Tian et al. (*20*). Aniline and 3CP were purchased from Aldrich, while $[Co(NH_3)_5Cl]^{2+}$ was synthesized (*21*). The H39C;C102T mutant of yeast iso-1-Cc was prepared as described by Hilgen and Pielak (*22*). Wild-type yeast iso-1-Cc has a free cysteine at residue 102, which causes dimerization and is an undesirable location for ruthenium labeling. The C102T variant, which is structurally and functionally identical to the wild-type protein (*23*−*25*), is used to circumvent these problems. The horse K39C mutant was made with the Quikchange site-directed mutagenesis kit (Stratogene) with the primers GGCCTGTTCGGCCGGCTGCACGGCCAGGCGCCGGGC and GCCCGGCGCCTGGCCCGTGCAGCGGCCGAACAGGCC. The protein was expressed and purified from *E. coli* as described by Patel et al. (*26*).

Synthesis of Ru(2,2′-bipyrazine)$_2$(4-bromomethyl-4′-methyl-2,2′-bipyridine). [Ru(4-hydroxymethyl-4′-methyl-2,2′-bipyridine)Cl_4] was prepared from $RuCl_3 \cdot 3H_2O$ (Aldrich) and 4-hydroxymethyl-4′-methyl-2,2′-bipyridine (*27*) by the method described in ref *28*. [Ru(2,2′-bipyrazine)$_2$(4-hydroxymethyl-4′-methyl-2,2′-bipyridine)]$(PF_6)_2$ was synthesized from Ru(4-hydroxymethyl-4′-methyl-2,2′-bipyridine)Cl_4 and 2,2′-bipyrazine using the method described in ref *29*. Ru(2,2′-bipyrazine)$_2$(4-bromomethyl-4′-methyl-2,2′-bipyridine) was prepared by brominating [Ru(2,2′-bipyrazine)$_2$(4-hydroxymethyl-4′-methyl-2,2′-bipyridine)]$(PF_6)_2$ using the procedure described in ref *30*. The dry product was dissolved in a minimum of dry dimethylformamide and stored under nitrogen at −90 °C. The extinction coefficient was 12 000 M^{-1} cm^{-1} at 463 nm.

Preparation of Ru$_z$-39-Cc. H39C;C102T yeast iso-1-Cc (530 μM) was treated with 260 μM dithiothreitol in 50 mM sodium borate, pH 9.0, under anaerobic conditions for 15 min to reduce any cross-linked dimers, and then 1.8 mM Ru(bpz)$_2$(4-bromomethyl-4′-methylbipyridine) was added under anaerobic conditions and allowed to react for 3 h at 37 °C. The reaction mixture was exchanged into 5 mM sodium phosphate, pH 7.0, using Amicon concentrators to remove excess reagent, and the Ru$_z$-39-Cc derivative was purified using a Waters 625 HPLC equipped with a Waters 1 × 10 cm Sp 8HR cation exchange column as described previously (*30*). The yield of Ru$_z$-39-Cc was 70%. Horse Ru$_z$-39-Cc was prepared using the same methods from horse K39C Cc expressed in *E. coli*. The location of the ruthenium complex at Cys-39 was confirmed by tryptic digestion, HPLC separation of the resulting peptides, and sequencing the ruthenium labeled peptide, as previously described (*30*). The UV/visible spectrum of Ru$_z$-39-Cc was the sum of the spectra of 1 equiv of Ru(bpz)$_2$(dmb) and 1 equiv of native yeast iso-1-Cc, with no shifts in the absorption band maxima in either redox state.

Steady-State Assay for the Reaction between Cc and Cytochrome bc_1. The purified cyt bc_1 complex was diluted to a final cyt *b* concentration of 1 μM with buffer containing 50 mM sodium phosphate, pH 7.0, 250 mM sucrose, 0.2 mM EDTA, 1 mM NaN_3, and 0.01% lauryl maltoside. A total of 3 μL of diluted bc_1 complex was added to a 1-mL assay mixture containing 25 mM sodium phosphate buffer, pH 7.0, 0.3 mM EDTA, 150 mM NaCl, 25 μM $Q_0C_{10}Br$, $Q_0C_{10}BrH_2$, and 50 μM Cc. Steady-state activity was measured from the rate of reduction of Cc detected at 550 nm using a millimolar extinction coefficient of 18.5 cm^{-1}. The rate of nonenzymatic reduction of Cc by $Q_0C_{10}BrH_2$, determined under the same conditions in the absence of enzyme, was subtracted from the rate in the presence of enzyme. The turnover number of purified yeast cyt bc_1 was 150 s^{-1}. To compare the steady-state activity of Ru$_z$-39-Cc with that of the C102T yeast iso-1 control, the reaction was measured at low Cc concentrations down to 1 μM to determine the V_{max}/K_m parameter. Previous studies have shown that V_{max}/K_m is the steady-state parameter that is most sensitive to the interaction between Cc and cyt c_1 (*3*). Moreover, V_{max}/K_m is most sensitive to the interaction between Cc and cyt c_1 at high ionic strength where complex dissociation is not rate-limiting (*3*). The ionic strength used for the steady-state assay, 200 mM, was chosen to optimize the sensitivity to the interaction between the two cytochromes (*31*, *32*). The steady-state V_{max}/K_m value for yeast Ru$_z$-39-Cc with yeast cyt bc_1 was 100 ± 15% that of the yeast C102T iso-1-Cc control, indicating that the ruthenium complex did not affect the interaction with cyt bc_1. Likewise, the V_{max}/K_m parameter for horse Ru$_z$-39-Cc with bovine cyt bc_1 was 100 ± 15% that of native horse Cc.

Flash Photolysis Experiments. Transient absorbance measurements of internal electron transfer between ruthenium and heme in Ru$_z$-39-Cc were carried out as described by Durham et al. (*33*). Solutions contained 5−20 μM Ru$_z$-39-Cc in 300 μL of 5 mM sodium phosphate, pH 7.0, in semimicro glass cuvettes. The excitation pulse was provided by the third harmonic of a Nd:YAG laser, with a pulse width of 20 ns and wavelength of 356 nm. The probe source was a pulsed 75 W xenon arc lamp, and the photomultiplier detector had a response time of 10 ns. Transient absorbance measurements of the reaction between Ru$_z$-39-Cc and cyt bc_1 were carried out as described by Heacock et al. (*34*) by flash photolysis of 300-μL solutions contained in a 1-cm glass semimicrocuvette. The excitation light pulse was provided by a phase R model DL1400 flash lamp-pumped dye laser using coumarin LD 490 to produce a 480 nm light flash of <0.5 μs duration. The detection system has been described by Heacock et al. (*34*). The reactions of Cc and cyt c_1 were monitored over the wavelength range of 540−560 nm using samples containing 3−6 μM cyt bc_1, 3−10 μM Ru$_z$-39-Cc, 0.01% lauryl maltoside in 5 mM sodium phosphate, pH 7.0, and 0−800 mM NaCl. 10 μM sodium ascorbate and 2 μM TMPD were added to reduce cyt c_1 and Ru$_z$-39-Cc, and 0.5 mM sodium cyanide was added to inhibit a small amount of cytochrome oxidase present in the yeast cyt bc_1 preparation. The oxygen in air-saturated buffer oxidized Ru(I) and prevented the back reaction. All absorbance transients were analyzed using the KINFIT kinetics program obtained from On-line Instrument Systems Inc. The absorbance spectra were obtained with a Hewlett-Packard 8452A diode array spectrophotometer.

RESULTS

Preparation and Characterization of Ru$_z$-39-Cc. To study rapid electron transfer from cyt bc_1 to Cc in the forward, physiological direction, it is necessary to have a ruthenium

Scheme 1

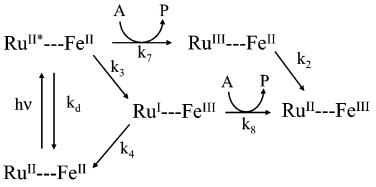

Table 1: Standard Reduction Potentials of Ruthenium Complexes[a]

complex	(III)/(II)	(III)/(II*)	(II)/(I)	(II*)/(I)
$Ru(bpy)_3$	1.27	−0.87	−1.31	0.83
$Ru(bpy)_2(dmb)$	1.27	−0.83	−1.36	0.79
$Ru(bpz)_2(dmb)$	1.76	−0.25	−0.79	1.22
$Ru(bpd)_2(dmb)$	1.49	−0.49	−1.00	0.98
$Ru(bpm)_2(dmb)$	1.55	−0.30	−0.95	0.90

[a] The potentials for (III)/(II) and (II)/(I) were measured in acetonitrile at 20 °C with respect to a saturated calomel reference electrode (*29*, *36*, *53*, *54*). The potentials for (III)/(II*) and (II*)/(I) were calculated from the ground-state potentials and the emission energies, determined at 77 K in ethylene glycol/water frozen glass (*53*, *54*).

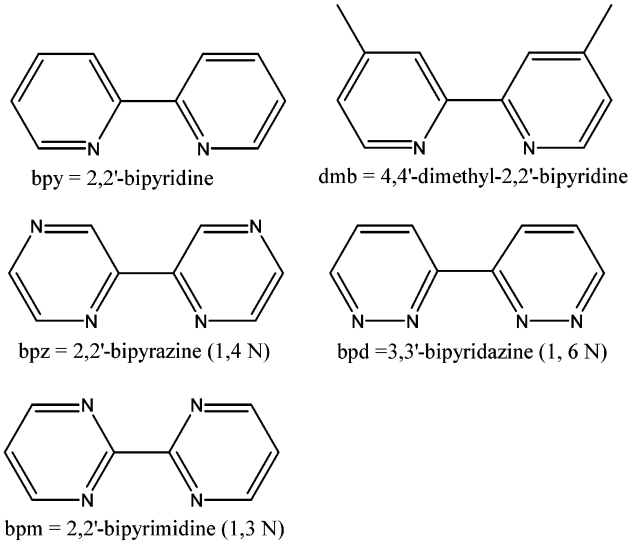

complex that will photooxidize the ferrous heme in Cc. The $Ru(bpy)_2(dmb)$ complex used in previous biological electron-transfer studies is not able to photooxidize Cc in sufficient yield (*30*, *35*). We therefore designed a new complex, $Ru(bpz)_2(dmb)$, which has a large reduction potential for the Ru(II*)/Ru(I) transition and should efficiently photooxidize heme *c* according to Scheme 1 (Table 1). The new $Ru(bpz)_2$-(4-bromomethyl-4′-methylbipyridine) reagent was synthesized and used to label the single sulfhydryl group on H39C;C102T yeast Cc to form Ru_z-39-Cc. The steady-state activity of yeast Ru_z-39-Cc with yeast cyt bc_1 was compared with that of C102T yCc at 200 mM ionic strength, where the V_{max}/K_m parameter is maximally sensitive to the reaction between Cc and cyt c_1 (*3*, *31*). The V_{max}/K_m parameter of yeast Ru_z-39-Cc was 100 ± 15% of the value for the C102T yCc control, indicating that the ruthenium complex does not interfere in the interaction with cyt c_1. The steady-state V_{max}/K_m parameter of horse Ru_z-39-Cc with bovine cyt bc_1 was 100 ± 15% as compared to the activity of native horse Cc under the same conditions.

Interprotein Electron Transfer in Ru_z-39-Cc. Transient absorption measurements were carried out on Ru_z-39-Cc to study electron transfer between the ruthenium complex and

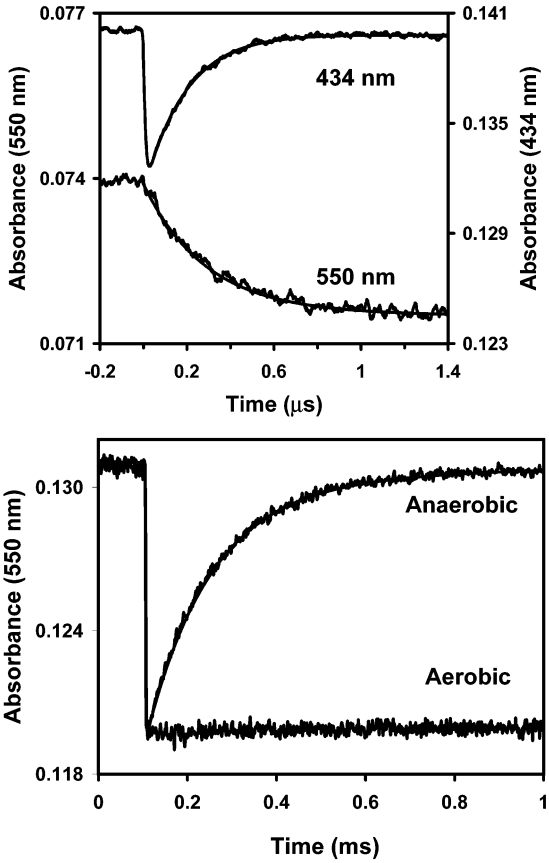

FIGURE 2: Photoinduced electron transfer within yeast Ru_z-39-Cc. A solution containing 5 μM Ru_z-39-Cc in 5 mM sodium phosphate, pH 7.0, was treated with 2 μM TMPD and 20 μM ascorbate to reduce the heme group. (A) The sample was photoexcited with a 356 nm Nd:YAG laser flash of 20 ns duration, and the absorbance at 434 and 550 nm was monitored with the fast detection system. The 434 nm transient represents the photoexcitation and recovery of Ru(II), while the 550 nm transient shows the photooxidation of the reduced heme. (B) The same sample as in panel A was photoexcited with the 480 nm flashlamp-pumped dye laser, and the absorbance was monitored with the intermediate detection system. Signals were recorded in the presence and absence of atmospheric oxygen. The solid lines at both wavelengths in panels A and B represent the best fit of Scheme 1 to the transients, with $k_3 = (1.5 \pm 0.2) \times 10^6\ s^{-1}$, $k_4 = 7000 \pm 1000\ s^{-1}$, and $k_d = (3.5 \pm 0.6) \times 10^6\ s^{-1}$, using the equations and methods given in Durham et al. (*33*).

the heme. Flash photolysis of reduced yeast Ru_z-39-Cc under anaerobic conditions resulted in electron transfer from reduced heme Fe(II) to photoexcited Ru(II*) to form Ru(I) and Fe(III) (Figure 2A). The initial formation and decay of Ru(II*) was detected at 434 nm, an isobestic for the Cc heme, while the oxidation of Fe(II) was detected at 550 nm. On a longer time scale, the thermal back reaction from Ru(I) to Fe(III) was observed with a rate constant of $k_4 = 7000 \pm 1000\ s^{-1}$ (Figure 2B). A unique set of values, $k_3 = (1.5 \pm 0.2) \times 10^6\ s^{-1}$, $k_4 = 7000 \pm 1000\ s^{-1}$, and $k_d = (3.5 \pm 0.6) \times 10^6\ s^{-1}$, were required to fit the 550 and 434 nm transients to the mechanism of Scheme 1, using the equations and procedures described in Durham et al. (*33*). These values were independent of protein concentration from 1 to 10 μM, indicating that they represent intraprotein electron transfer. When the solution was oxygenated with air, the initial electron transfer from Fe(II) to Ru(II*) occurred with the same rate constant as observed under anaerobic conditions, but the back electron-transfer reaction from Ru(I) to Fe(III)

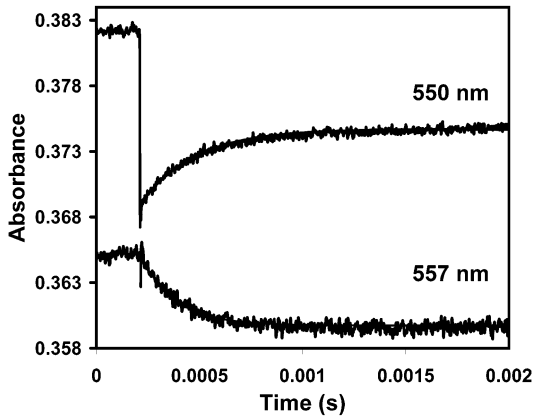

FIGURE 3: Photoinduced electron transfer between yeast Ru-39-Cc and yeast cyt bc_1. A solution containing 5.2 μM yeast Ru_z-39-Cc and 4.4 μM yeast cyt bc_1 in 5 mM sodium phosphate, pH 7.0, 250 mM NaCl, and 0.1% lauryl maltoside was treated with 2 μM TMDP and 10 μM ascorbate to reduce the c_1 and c hemes and photoexcited with a 480 nm laser flash of 500 ns duration. Cc photooxidation and reduction was monitored at 550 nm, and cyt c_1 oxidation was monitored at 557 nm. The rate constants for the exponential transients at both wavelengths were 3900 $\pm$ 600 s^{-1}.

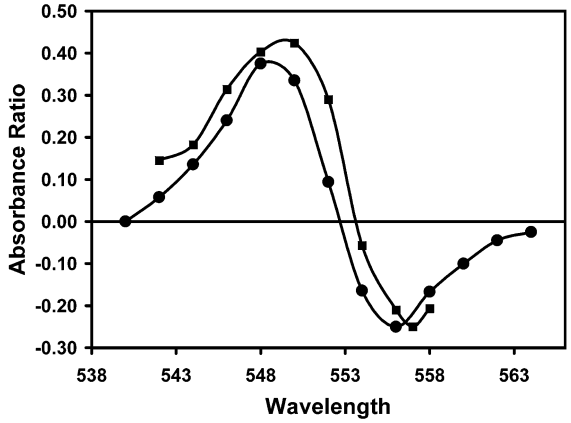

FIGURE 4: Kinetic difference spectrum for photoinduced electron transfer between Ru_z-39-Cc and cyt bc_1. (■) Absorbance transients were recorded for the reaction between yeast Ru_z-39-Cc and yeast cyt bc_1 under the conditions of Figure 3. The absorbance ratio is the ratio of the transient absorbance change at the indicated wavelength to the initial absorbance decrease at 550 nm. (●) Absorbance transients were recorded for the reaction between horse Ru_z-39-Cc and bovine cyt bc_1 under the same conditions as Figure 3, except that the NaCl concentration was 120 mM.

was prevented (Figure 2B), indicating that Ru(I) was oxidized by oxygen in the solution. The back reaction could also be prevented under anaerobic conditions by adding $[Co(NH_3)_5Cl]^{2+}$ to the solution, which irreversibly oxidizes Ru(I) (*36*).

Electron Transfer between Ru_z-39-Cc and Cyt c_1 in the Cytochrome bc_1 Complex. The rapid photooxidation of the reduced heme in Ru_z-39-Cc makes it possible to study electron transfer from cyt c_1 in the cyt bc_1 complex to Cc in the forward, physiological direction. Flash photolysis of reduced yeast cyt bc_1 and yeast Ru_z-39-Cc in 260 mM ionic strength buffer resulted in rapid photooxidation of Fe(II) by Ru(II*) in Ru_z-39-Cc, as indicated by the decrease in 550 nm absorbance (Figure 3). The rapid decrease in 550 nm absorbance was followed by an exponential increase with a rate constant of 3900 $\pm$ 600 s^{-1}, indicating electron transfer from cyt c_1 Fe(II) to heme Fe(III) in Ru_z-39-Cc (Figure 3). The oxidation of cyt c_1 was observed directly at 557 nm, which is an isobestic point for Cc. The rate constant for oxidation of cyt c_1 measured at 557 nm was the same as the rate constant for reduction of heme c measured at 550 nm, 3900 $\pm$ 600 s^{-1}. Transients recorded over the wavelength range of 540−560 nm all had the same rate constant and gave a kinetic difference spectrum with a maximum at 550 nm and a minimum at 557 nm (Figure 4), which is consistent with the difference spectrum for electron transfer from cyt c_1 to cyt c (*5*). The Rieske iron−sulfur protein is expected to partially rereduce cyt c_1 following oxidation under the conditions of Figure 3 (*2*, *37*). However, there was no difference in the kinetics of cyt c_1 oxidation and heme c reduction, suggesting that the rate constant for electron transfer from the iron−sulfur protein to cyt c_1 is much faster than the rate constant for electron transfer from cyt c_1 to heme c. Under these conditions, the iron−sulfur protein and cyt c_1 will remain in rapid equilibrium with each other as electron transfer from cyt c_1 to heme c occurs. The rate constant for electron transfer between the iron−sulfur protein and cyt c_1 has been measured to be 80 000 s^{-1} in *R. sphaeroides* and bovine cyt bc_1 (*37*) but has not been measured in yeast cyt bc_1 (*38*).

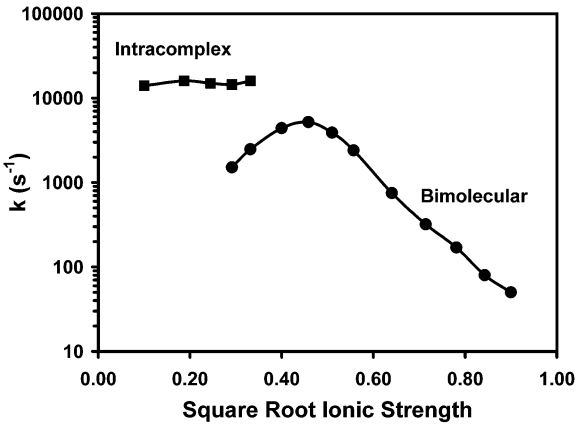

FIGURE 5: Ionic strength dependence of the rate constant for photoinduced electron transfer between yeast Ru_z-39-Cc and yeast cyt bc_1. Solution containing 5.2 μM yeast Ru_z-39-Cc and 4.4 μM yeast cyt bc_1 in 5 mM sodium phosphate, pH 7.0, 0−800 mM NaCl, and 0.1% lauryl maltoside was treated with 2 μM TMDP and 10 μM ascorbate to reduce the c_1 and c hemes and photoexcited with a 480 nm laser flash. The rate constants for electron transfer from cyt c_1 to heme c were measured at 557 and 550 nm as described in Figure 3. (■) Fast intracomplex phase. (●) Slow bimolecular phase.

The rate constant for electron transfer from cyt c_1 to Ru_z-39-Cc decreased with increasing ionic strength above 250 mM ionic strength, consistent with a reaction between oppositely charged proteins (Figure 5). At 250 mM ionic strength and above, the rate constant was linearly dependent on the protein concentration, consistent with a bimolecular reaction between solution cyt bc_1 and solution Ru_z-39-Cc with a second-order rate constant k_{2nd} (Figure 6). The pseudo-first-order rate constant reached a maximum of 5200 $\pm$ 1000 s^{-1} as the ionic strength was decreased to 210 mM. When the ionic strength was decreased to 110 mM the transient became biphasic, with a slow bimolecular phase with a rate constant of 2500 $\pm$ 500 s^{-1} and a relative amplitude of 40%, and a fast phase with a rate constant of 14 000 $\pm$ 3000 s^{-1} and a relative amplitude of 60% (Figure 5). As the ionic strength was decreased below 75 mM, the slow phase disappeared, and only a fast monophasic transient was

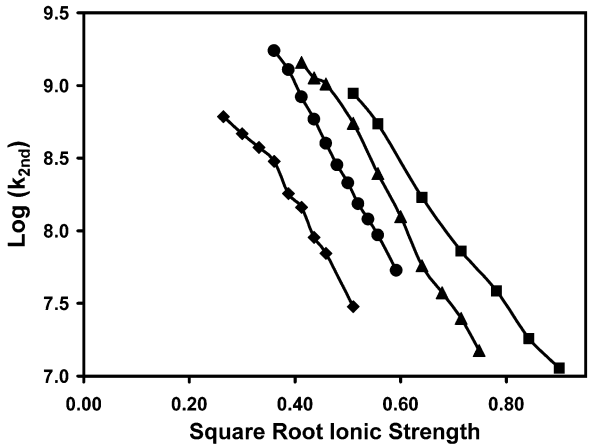

FIGURE 6: Ionic strength dependence of the second-order rate constant for electron transfer between Ru_z-39-Cc and cyt bc_1. The rate constants were measured as described in Figure 5 to obtain the second-order rate constants. (■) Yeast Ru_z-39-Cc with yeast cyt bc_1. (●) Horse Ru_z-39-Cc with bovine cyt bc_1. (▲) Yeast Ru_z-39-Cc with bovine cyt bc_1. (◆) Horse Ru_z-39-Cc with yeast cyt bc_1.

Scheme 2

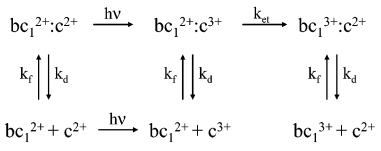

Scheme 3

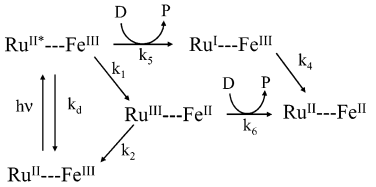

observed (Figure 5). The rate constant of the fast phase was independent of ionic strength from 5 to 110 mM (Figure 5) and also independent of protein concentration, indicating that it represented electron transfer from cyt c_1 to photooxidized Ru_z-39-Cc within a 1:1 complex between the two proteins. The results at all ionic strengths are consistent with Scheme 2, in which electron transfer occurs within a preformed complex at low ionic strength, while at high ionic strength uncomplexed Ru_z-39-Cc must first bind to cyt bc_1 before intracomplex electron transfer can take place. Reverse electron transfer from Cc to cyt bc_1 was studied using yeast Ru_p-39-Cc, which is rapidly photoreduced according to Scheme 3 (*30*). Aniline and 3CP were used as sacrificial electron donors to reduce Ru(III) and prevent the back reaction. Flash photolysis was carried out in solutions containing 5 μM oxidized Ru_p-39-Cc, 5 μM yeast cyt bc_1 in 5 mM sodium phosphate, pH 7.0, 0.1% lauryl maltoside, 10 mM aniline, and 1 mM 3CP. Upon photoreduction of the heme *c* in Ru_p-39-Cc, electron transfer from heme *c* Fe(II) to cyt c_1 Fe(III) was observed with a rate constant of 14 000 $\pm$ 4000 s^{-1}. This rate constant at low ionic strength was independent of protein concentration, consistent with intracomplex electron transfer. The rate constant remained the same as the ionic strength and was increased up to 100 mM, and then the fast intracomplex phase was replaced by a slow bimolecular phase. The ionic strength dependence of the

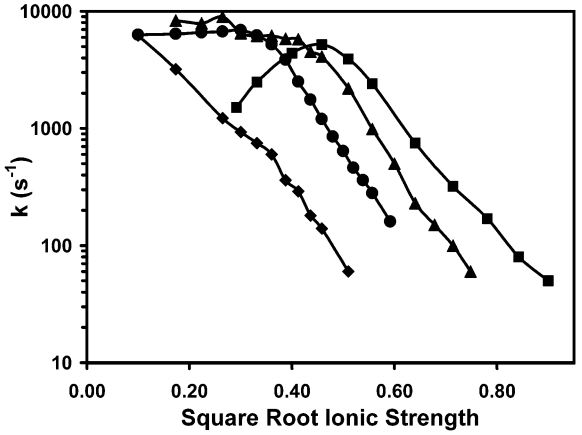

FIGURE 7: Ionic strength dependence of the rate constant for photoinduced electron transfer between Ru_z-39-Cc and cyt bc_1. The rate constants were measured as described in Figure 5. (■) Yeast Ru_z-39-Cc with yeast cyt bc_1. (●) Horse Ru_z-39-Cc with bovine cyt bc_1. (▲) Yeast Ru_z-39-Cc with bovine cyt bc_1. (◆) Horse Ru_z-39-Cc with yeast cyt bc_1.

bimolecular phase was similar to that for Ru_z-39-Cc (data not shown).

The reaction between bovine cyt bc_1 and horse Ru_z-39-Cc was studied to characterize a mammalian system. At 5 mM ionic strength, the rate constant for electron transfer from cyt c_1 to heme *c* in photooxidized horse Ru_z-39-Cc was 6300 $\pm$ 1500 s^{-1}, independent of protein concentration. The kinetics changed very little as the ionic strength was increased to 90 mM ionic strength, where the transient was monophasic with a rate constant of 6900 $\pm$ 1500 s^{-1} (Figure 7). The wavelength dependence of the transient was similar to that seen for the reaction between yeast Ru_z-39-Cc and yeast cyt bc_1 (Figure 4). There was no difference in the rate constant for cyt c_1 oxidation and cyt *c* reduction and thus no indication of electron transfer between the iron−sulfur center and cyt c_1. Increasing the ionic strength above 100 mM resulted in a decrease in the rate constant of the monophasic transient. The rate constant was linearly dependent on protein concentration above 120 mM ionic strength, indicating a second-order reaction between solution cyt bc_1 and photooxidized Ru_z-39-Cc (Figure 6). These results indicate that electron transfer occurs within a 1:1 complex between cyt bc_1 and Ru_z-39-Cc at ionic strengths below 80 mM, and the complex dissociates at about 80 mM ionic strength. It is apparent from the ionic strength dependence that the complex between horse Ru-39-Cc and bovine cyt bc_1 dissociates at a much lower ionic strength than the corresponding complex between yeast Ru_z-39-Cc and yeast cyt bc_1. To determine whether the difference in binding affinity is due primarily to the Cc or cyt bc_1 component, various combinations were investigated. The reaction between yeast Ru_z-39-Cc and bovine cyt bc_1 was similar to that between the two yeast proteins. The rate constant for electron transfer between cyt c_1 and heme *c* was 8300 $\pm$ 1200 s^{-1} at low ionic strength and remained nearly the same up to 200 mM ionic strength (Figure 7). Further increases in ionic strength led to a decrease in the rate constant. In contrast, the interaction of horse Ru_z-39-Cc with yeast cyt bc_1 was quite a bit weaker than that of yeast Ru_z-39-Cc. The rate constant was 6200 $\pm$ 1000 s^{-1} at 5 mM ionic strength and decreased as the ionic strength was increased to 20 mM and higher (Figure 7). The ionic strength

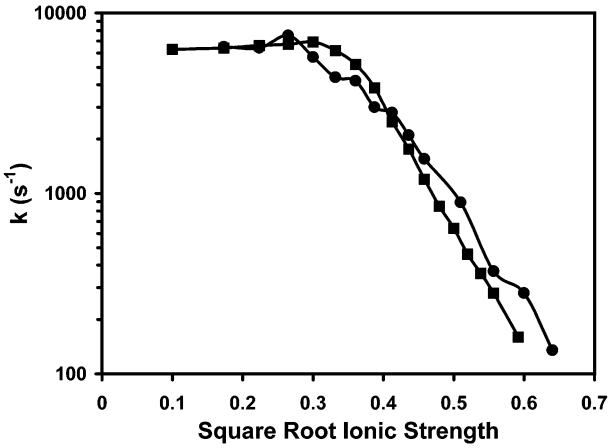

FIGURE 8: Ionic strength dependence of the rate constant for photoinduced electron transfer between yeast Ru_z-39-Cc and *R. sphaeroides* cyt bc_1. The rate constants were measured as described in Figure 5. (●) Yeast Ru_z-39-Cc with *R. sphaeroides* cyt bc_1. (■) Horse Ru_z-39-Cc with bovine cyt bc_1.

dependence of the reaction of yeast Ru_z-39-Cc with *R. sphaeroides* cyt bc_1 was similar to that of bovine cyt bc_1 (Figure 8).

DISCUSSION

Design of Ru_z-39-Cc for Rapid Electron Transfer between Ruthenium and Heme c. Steady-state spectroscopic studies of the reaction between Cc and cyt bc_1 have shown that the V_{max}/K_m parameter decreases with increasing ionic strength, consistent with a reaction between oppositely charged proteins (*3*, *4*, *7*). Stopped-flow spectroscopy has been used to measure electron transfer between Cc and cyt c_1 at high ionic strength, where a second-order reaction between the two molecules in solution is observed (*5*, *6*, *39*). However, the reaction becomes too fast to resolve by stopped-flow spectroscopy as the ionic strength is decreased below 200 mM. The reaction has also been studied in *R. sphaeroides* chromatophores, where the reaction is limited by the diffusion of photooxidized cyt c_2 from the reaction center to the cyt bc_1 complex with an apparent rate constant of 5000 s^{-1} (*40*−*42*). The techniques discussed above have provided important information about the nature of the reaction between cyt c_1 and Cc but have not been used to measure the intracomplex rate constant. In the only previous studies of intracomplex electron transfer between cyt c_1 and Cc, the reaction between horse Ru-72-Cc and bovine cyt bc_1 was found to occur with an intracomplex rate constant of 6×10^4 s^{-1} (*34*, *43*). However, there were several features of the Ru-72-Cc derivative that raise the question of how well the measured rate constant reflects the true rate constant in the native complex. The steady-state V_{max}/K_m parameter for the reaction of Ru-72-Cc with cyt bc_1 was 4.5-fold smaller than that of native horse Cc, indicating that the binding strength and orientation of the complex is affected by the ruthenium complex at lysine 72 near the heme crevice (*43*). Moreover, it was only possible to measure electron transfer in the Cc to cyt c_1 direction with Ru-72-Cc, which is the reverse of the physiological direction of electron transfer.

The new yeast Ru_z-39-Cc derivative was designed to reliably measure intracomplex electron transfer with the cyt bc_1 complex in the physiological direction. The ruthenium complex is attached to Cys-39 on the surface opposite from the heme crevice of Cc, where it should not affect the interaction with cyt bc_1 (Figure 1). The steady-state V_{max}/K_m parameter for the reaction of yeast Ru_z-39-Cc with yeast cyt bc_1 is the same as that of the C102T yCc control, providing evidence that the ruthenium complex does not affect the binding strength or orientation of the complex with cyt bc_1. There is an efficient pathway for electron transfer between the ruthenium complex attached to Cys-39 and the heme group consisting of 13 covalent bonds and one hydrogen bond (*30*). The closest distance between the heme macrocycle and the $Ru(bpz)_2(dmb)$ complex is 12.6 Å. Of all the ruthenium complexes investigated, the newly developed $Ru(bpz)_2(dmb)$ complex has the largest reduction potential for the Ru(II*)/Ru(I) transition and should be optimized for photooxidation of the reduced heme *c* (Table 1). Laser excitation of the reduced Ru_z-39-Cc derivative resulted in electron transfer from heme *c* Fe(II) to Ru(II*) with a rate constant of $k_3 = 1.5 \times 10^6$ s^{-1}, followed by back electron transfer from Ru(I) to Fe(III) with a rate constant of $k_4 = 7000$ s^{-1}. The driving force of the Ru(II*)-Fe(II) → Ru(I)-Fe(III) reaction (1.0 V) is close to the expected reorganization energy λ of 0.8 V for electron transfer, allowing a maximal rate of electron transfer (Table 1). It is not clear why the back electron-transfer reaction from Ru(I) to Fe(III) in Ru_z-39-Cc is so slow, $k_2 = 7000$ s^{-1}, since the driving force for this reaction should also be about 1.0 V (Table 1). It should be noted that the reduction potentials in Table 1 were measured in acetonitrile and may be somewhat different in aqueous solution. In any case, the slow back reaction is advantageous for the present experiments since it can be easily prevented by atmospheric oxygen, which oxidizes Ru(I). The yield of photooxidized heme *c* is 20% in a single flash, which is quite large for this type of derivative. The high yield is important for the electron-transfer studies with cyt bc_1 because the spectra of Cc and cyt c_1 are very similar in the α region, leading to small absorbance changes upon electron transfer.

Electron Transfer between Ru_z-39-Cc and Cytochrome bc_1. Flash photolysis of a 1:1 complex between yeast Ru_z-39-Cc and yeast cyt bc_1 at low ionic strength results in intracomplex electron transfer from cyt c_1^{2+} to photooxidized heme c^{3+} with a rate constant of 14 000 ± 3000 s^{-1}. The rate constant of this phase was independent of ionic strength from 5 to 100 mM, indicating that the complex does not change its configuration over this ionic strength range. The same intracomplex rate constant was also obtained for the reverse reaction between photoreduced heme *c* and oxidized cyt c_1 using the Ru_p-39-Cc derivative. This indicates that electron transfer between cyt c_1 and cyt *c* is fully reversible, consistent with the fact that the redox potentials of the two cytochromes are nearly the same. It is of interest to interpret the experimental rate constant for electron transfer in the context of the X-ray crystal structure of the complex between yeast iso-1-Cc and yeast cyt bc_1 (*17*, *32*) (Figure 1). In the crystallographic complex, the heme *c* and heme c_1 groups are in close proximity with their pyrrol C rings oriented toward each other. The iron atoms of the two heme groups are separated by 17.4 Å, while the edge-to-edge distance between the two porphyrin heterocycles is 9.4 Å. Dutton and co-workers have reported that electron transfer rate constants in a broad range of biological systems can be described

approximately by a simple exponential dependence on the distance between the redox centers, as originally proposed by Marcus (*44*):

$$k_{et} = k_o \exp[-\beta(r - r_o)] \exp[(-(\Delta G^{\circ\prime} + \lambda)^2/4\lambda RT)] \quad (1)$$

where r is the distance between the closest macrocycle atoms in the two redox centers, the van der Waals contact distance $r_o = 3.6$ Å, $\beta = 1.4$ Å^{-1}, and the nuclear frequency $k_o = 10^{13}$ s^{-1}. Assuming an edge-to-edge separation of 9.4 Å between the cyt c_1 and Cc hemes, and a reorganization energy λ between 0.7 and 1.0 V, the rate constant estimated from eq 1 is between 1.8×10^5 s^{-1} and 3.3×10^6 s^{-1}. This estimated value is larger than the experimental value of 1.4×10^4 s^{-1} obtained with Ru$_z$-39-Cc in the present experiments. However, the theory has been applied most extensively to intraprotein electron transfer, with relatively few applications to intracomplex electron transfer between two proteins. The rate constant is expected to be sensitive to the specific environment between the two hemes, and a through-space jump of 4.5 Å between the CBC groups of the two hemes as postulated in the Cc−bc_1 complex could give a lower rate constant than that estimated from eq 1. Application of the pathway theory developed by Beratan and Onuchic (*45*) to this system gives a predicted rate constant of just 500 s^{-1}, assuming a pathway consisting of four covalent bonds connecting the heme macrocycles to the CBC groups and a through-space jump of 4.5 Å between the heme CBC groups. Of course, it is likely that the gap between the CBC groups is occupied by water molecules, which would help mediate electron transfer. Nevertheless, these estimations point out the difficulty of predicting interprotein electron transfer. It is also possible that the yCc:bc_1 complex assumes a slightly different orientation in solution than in the crystal. An increase in the heme−heme separation from 9.4 to just 11.0 Å would decrease the rate constant calculated from eq 1 to 1.5×10^4 s^{-1}, the same as the experimental value. The complex might also fluctuate between several different configurations in solution, in which case the rate constant for electron transfer could be controlled by configurational gating (*46*).

When the ionic strength is increased to 110 mM, the amplitude of the fast intracomplex phase of electron transfer decreases, and a slow phase with a rate constant of 2500 s^{-1} appears due to the bimolecular reaction of solution Ru$_z$-39-Cc with cyt bc_1 (Figure 5). The relative amplitudes of the fast and slow phases are 60 and 40%, respectively, indicating that the 1:1 complex is 40% dissociated, and the equilibrium dissociation constant is $K_d = 0.85$ μM. The presence of both intracomplex and bimolecular phases at this ionic strength indicates that the bimolecular reaction involves formation of a 1:1 complex followed by intracomplex electron-transfer according to Scheme 2 with $k_d \ll k_{et}$ (*43*, *47*). The observed rate constant of the bimolecular phase is given by eq 2:

$$k_{obs} = k_f(E_o - {}^1/_2(k_d/k_f + E_o + C_o - ((k_d/k_f + E_o + C_o)^2 - 4E_oC_o)^{1/2})) \quad (2)$$

where E_o is the concentration of cyt bc_1, and C_o is the concentration of Ru$_z$-39-Cc (*43*, *47*). From this equation, the formation and dissociation rate constants can be estimated to be $k_f = 2.0 \times 10^9$ M^{-1} s^{-1} and $k_d = 1.7 \times 10^3$ s^{-1}, using the relation $K_d = k_d/k_f$. As the ionic strength is increased to 200 mM, the rate constant k_{obs} increases to a maximum, and the fast intracomplex phase disappears, indicating an increase in k_d and complex dissociation. The maximum in the bimolecular phase of electron transfer for Ru$_z$-39-Cc occurs at the same ionic strength, 200 mM, as the maximum in the steady-state assay using native yeast Cc (*31*, *32*). The second-order rate constant decreases with increasing ionic strength above 250 mM, consistent with a reaction between oppositely charged proteins (Figure 6) (*4*). Even though there is only one electrostatic charge-pair interaction in the binding domain of the yCc:ybc_1 crystallographic complex, there are five lysine amino groups on yCc and five carboxylate groups on cyt bc_1 immediately surrounding the interaction domain, which could contribute to complex formation between the two proteins (Figure 1). These residues may help guide Cc to the correct binding site during the final stages of the complex formation process.

The intracomplex rate constant for electron transfer between horse Ru$_z$-39-Cc and bovine cyt bc_1 was 6300 ± 1500 s^{-1} at 5 mM ionic strength and remained nearly the same up to 85 mM ionic strength (Figure 7). This value is smaller than that for the reaction between yeast Ru$_z$-39-Cc and yeast cyt bc_1, 14 000 ± 3000, which could be due to a slight difference in the orientation of the two complexes. Above 120 mM ionic strength the reaction rate decreased as the complex dissociated, and the reaction became bimolecular. Separate intracomplex and bimolecular phases were not observed at intermediate ionic strength, indicating that the dissociation rate constant k_d becomes comparable to k_{et} as the complex begins to dissociate, and rapid equilibrium conditions apply. The reaction rate k_{obs} measured for Ru$_z$-39-Cc begins to decrease at the same ionic strength, 120 mM, as the V_{max}/K_m parameter determined for native horse Cc by steady-state kinetics (*3*). This indicates that Ru$_z$-39-Cc dissociates from cyt bc_1 at the same ionic strength as native horse Cc, consistent with the identical steady-state activities of the two cytochromes.

The horse Ru$_z$-39-Cc−bovine bc_1 complex dissociates at a lower ionic strength than the yeast Ru$_z$-39-Cc−yeast bc_1 complex, but the slope of the plot of the second-order rate constant versus ionic strength is similar for the two systems. These results suggest that the complex is stronger in the yeast system because of more favorable hydrophobic contacts but that the electrostatic interactions are similar in the two systems. It is interesting to compare the reactions of the different combinations of Cc and cyt bc_1 species. Yeast Ru$_z$-39-Cc interacted more strongly with bovine cyt bc_1 than did horse Ru$_z$-39-Cc, with an intracomplex rate constant of 8000 s^{-1} at low ionic strength, which remained nearly constant up to 160 mM ionic strength (Figure 7). In contrast, the interaction of horse Ru$_z$-39-Cc with yeast cyt bc_1 was much weaker than that of yeast Ru$_z$-39-Cc. The rate constant k_{obs} began to decrease as soon as the ionic strength was increased to 20 mM, indicating dissociation of the complex (Figure 7). The steady-state reaction of horse Cc with yeast cyt bc_1 also began to decrease from its optimum value at only 33 mM ionic strength, as compared to 220 mM ionic strength for yeast Cc (*31*). These results indicate that yeast Cc has a much stronger hydrophobic interaction with both yeast and bovine cyt bc_1 than does horse Cc. However, the electrostatic interactions of the two cytochromes *c* are similar, as indicated

by the similar slopes in the rate constant versus ionic strength plots (Figure 7). This is comparable to the situation with yeast cytochrome *c* peroxidase, where yeast Cc has a much stronger hydrophobic interaction than horse Cc (*48*). The origin of this difference between yeast and horse Cc is unknown. Most residues surrounding the heme domain of Cc are the same in horse and yeast, or are conservative substitutions (*49*). Significant differences include an Arg-13 in yCc as compared with Lys-13 in hCc, and a trimethyl Lys-72 in yCc as compared with Lys-72 in hCc. The planar stacking interaction between yCc Arg-13 and cyt c_1 Phe-230 may be a significant source of the stronger interaction for yCc.

Several electron transfer complexes share a common binding motif consisting of a central nonpolar contact domain surrounded by a peripheral electrostatic domain containing oppositely charged residues on the two proteins. These complexes include the *R. sphaeroides* cyt c_2:reaction center complex (*50*), the Cc:cyt *c* peroxidase complex (*35*, *47*, *48*, *51*), and the Cc:cyt *c* oxidase complex (*52*) in addition to the Cc:cyt bc_1 complex (*17*). The peripheral electrostatic interactions may guide the docking of Cc to the specific configuration stabilized by the central nonpolar domain that is optimized for rapid electron transfer.

REFERENCES

1. Trumpower, B. L., and Gennis, R. B. (1994) *Annu. Rev. Biochem. 63*, 675−716.
2. Trumpower, B. L. (1990) *J. Biol. Chem. 265*, 11409−11412.
3. Ahmed, A. J., Smith, H. T., Smith, M. B., and Millett, F. (1978) *Biochemistry 17*, 2479−2483.
4. Smith, H. T., Ahmed, A. J., and Millett, F. (1981) *J. Biol. Chem. 256*, 4984−4990.
5. Yu, C. A., Yu, L., and King, T. E. (1973) *J. Biol. Chem. 248*, 528−533.
6. Yu, C. A., Steidl, J. R., and Yu, L. (1983) *Biochim. Biophys. Acta 736*, 226−234.
7. Speck, S. H., Ferguson-Miller, S., Osheroff, N., and Margoliash, E. (1979) *Proc. Natl. Acad. Sci. U.S.A. 76*, 155−159.
8. König, B. W., Osheroff, N., Wilms, J., Muijsers, A. O., Dekker, H. L., and Margoliash, E. (1980) *FEBS Lett. 111*, 395−398.
9. Rieder, R., and Bosshard, H. R. (1980) *J. Biol. Chem. 255*, 4732−4739.
10. Stonehuerner, J., O'Brien, P., Geren, L., and Millett, F. (1985) *J. Biol. Chem. 260*, 5392−5398.
11. Gutweniger, H. E., Grassi, C., and Bisson, C. (1983) *Biochem. Biophys. Rev. Commun. 116*, 272−283.
12. Broger, C., Salardi, S., and Azzi, A. (1983) *Eur. J. Biochem. 131*, 349−352.
13. Xia, D., Yu, C.-A., Kim, H., Xia, J.-Z., Kachurin, A. M., Zhang, L., Yu, L., and Deisenhofer, J. (1997) *Science 277*, 60−66.
14. Zhang, Z., Huang, L., Shulmeister, V. M., Chi, Y.-I., Kim, K. K., Hung, L.-W., Crofts, A. R., Berry, E. A., and Kim, S.-H. (1998) *Nature 392*, 677−684.
15. Iwata, S., Lee, J. W., Okada, K., Lee, J. K., Wata, M., Rasmussen, B., Link, T. A., Ramaswamy, S., and Jap, B. K. (1998) *Science 281*, 64−71.
16. Hunte, C., Koepke, J., Lange, C., Rossmanith, T., and Michel, H. (2000) *Structure (London) 8*, 669−684.
17. Lange, C., and Hunte, C. (2002) *Proc. Natl. Acad. Sci. U.S.A. 99*, 2800−2805.
18. Snyder, C. H., and Trumpower, B. L. (1999) *J. Biol. Chem. 274*, 31209−31216.
19. Yu, C.-A., Xia, J.-Z., Kachurin, A. M., Yu, L., Xia, D., Kim, H., and Deisnenhofer, J. (1996) *Biochim. Biophys. Acta 1275*, 47−53.
20. Tian, H., Yu, L., Mather, M., and Yu, C. A. (1998) *J. Biol. Chem. 273*, 27953−27959.
21. Moeller, T., Ed. (1957) *Inorganic Synthesis*, Vol. V, p 185, McGraw Hill Book Company, Inc., New York.
22. Hilgen, S. E., and Pielak, G. J. (1991) *Protein Eng. 5*, 575−578.
23. Berghuis, A. M., and Brayer, G. D. (1992) *J. Mol. Biol. 223*, 959−976.
24. Cutler, R. L., Pielak, G. J., Mauk, A. G., and Smith, M. (1987) *Protein Eng. 1*, 95−99.
25. Gauo, Y., Boyd, J., Williams, R. J. P., and Pielak, G. J. (1990) *Biochemistry 29*, 6994−7003.
26. Patel, C. N., Lind, M. C., and Pielak, G. H. (2001) *Protein Expression Purif. 22*, 320−324.
27. Geren, L., Hahm, S., Durham, B., and Millett, F. (1991) *Biochemistry 30*, 9450−6457.
28. Krause, R. A. (1977) *Inorg. Chim. Acta 22*, 209−213.
29. Rillema, D. P., Allen, G., Meyer, T. J., and Conrad, D. (1983) *Inorg. Chem. 22*, 1617−1622.
30. Geren, L. M., Beasley, J. R., Fines, B. R., Saunders, A. J., Hibdon, S., Pielak, G. J., Durham, B., and Millett, F. (1995) *J. Biol. Chem. 270*, 2466−2472.
31. Schopink, T. J., Hemrika, W., and Berden, J. A. (1989) *Biochim. Biophys. Acta 974*, 192−201.
32. Hunte, C., Solmaz, S., and Lange, C. (2002) *Biochim. Biophys. Acta 1555*, 21−28.
33. Durham, B., Pan, L. P., Long, J., and Millett, F. (1989) *Biochemistry 28*, 8659−8665.
34. Heacock, C., Liu, R., Yu, C., Yu, L., Durham, B., and Millett, F. (1993) *J. Biol. Chem. 268*, 27171−27175.
35. Wang, K., Mei, H., Geren, L., Miller, M. A., Saunders, A., Wang, X., Waldner, J. L., Pielak, G. J., Durham, B., and Millett, F. (1996) *Biochemistry 35*, 15107−15119.
36. Kalyanasundaram, K. *Photochemistry of Polypyridine and Porphyrin Complexes* (1992) p 146, Academic Press, New York.
37. Sakoski, R. C., Engstrom, G., Tian, H., Zhang, L., Yu, C.-A., Yu, L., Durham, B., and Millett, F. (2000) *Biochemisry 39*, 4231−4236.
38. T'sai, A.-L., Olson, J. S., and Palmer, G. (1983) *J. Biol. Chem. 258*, 2122−2125.
39. Konig, B. W., Wilms, J., and Van Gelder, B. F. (1981) *Biochim. Biophys. Acta 636*, 9−16.
40. Meinhardt, S. W., and Crofts, A. R. (1982) *FEBS Lett. 149*, 223−227.
41. Snozzi, M., and Crofts, A. R. (1985) *Biochim. Biophys. Acta 809*, 260−270.
42. Crofts, A. R., and Wang, Z. (1989) *Photosynthesis Res. 22*, 69−87.
43. Tian, H., Sadoski, R., Zhang, L., Yu, C.-A., Yu, L., Durham, B., and Millett, F. (2000) *J. Biol. Chem. 275*, 9587−9595.
44. Moser, C. C., Keske, J. M., Warncke, K., Farid, R. S., and Dutton, P. L. (1992) *Nature 355*, 796−802.
45. Beratan, D. N., Betts, J. N., and Onuchic, J. N. (1992) *J. Chem. Phys. 96*, 2852−2855.
46. Davidson, V. L. (1996) *Biochemistry 35*, 14035−14039.
47. Mei, H., Wang, D., McKee, S., Wang, X., Pielak, G. J., Durham, B., and Millett, F. (1996) *Biochemistry 35*, 15800−15806.
48. Mei, H., Geren, L., Miller, M. A., Durham, B., and Millett, F. (2002) *Biochemistry 41*, 3968−3976.
49. Moore, G. R., and Pettigrew, G. W. (1990) *Cytochromes c: Evolutionary, Structural and Physicochemical Aspects*, Springer-Verlag, New York.
50. Axelrod, H. L., Abresch, E. C., Okamura, M. Y., Yey, A. P., Rees, D. C., and Feher, G. (2002) *J. Mol. Biol. 319*, 501−515.
51. Pelletier, H., and Kraut, J. (1992) *Science 258*, 1748−1755.
52. Wang, K., Zhen, Y., Sadoski, R., Grinnell, S., Geren, L., Ferguson-Miller, S., Durham, B., and Millett, F. (1999) *J. Biol. Chem. 274*, 38042−38050.
53. Scott, J. R., Willie, A., McLean, M., Stayton, P. S., Sligar, S. G., Durham, B., and Millett, F. (1993) *J. Am. Chem. Soc. 115*, 6820−6824.
54. Fairris, J. L., Wang, K., Geren, L., Pielak, G. J., Durham, B., and Millett, F. (1998) *Advances in Chemistry Series 254: 1998 Photochemistry and Radiation Chemistry*, pp 99−110, ACS, Washington, DC.

BI027213G